

Fig. S1. Schematic comparison of domain structures for the *Dictyostelium* DGKA and the 10 Human DGK isoforms. The *Dictyostelium* DGKA and the 10 human DGK isoforms are shown with amino acid number, the number and position of the phorbol-ester/ DAG type 1 binding domains (purple) and the catalytic site.

Dictyostelium discoideum (social amoeba) DGKA	330	MPEKVL	FVFN	SKSG	GQFG	STLIRKLS	SL	360	
Homo sapiens (human) DGK-alpha	372	PNTH	PLLVFN	PKSG	GKQG	QRVLWK	FQYI	402	
Homo sapiens (human) DGK-beta	434	PGTH	PLLVFN	PKSG	GKQG	GERIYRK	FQYL	464	
Homo sapiens (human) DGK-gamma	430	PGTH	PLLVFN	PKSG	GRQGER	ILRK	FHYL	460	
Homo sapiens (human) DGK-delta	317	SCTS	PLLVFN	SKSG	DNQGVK	FLRR	FKQL	347	
Homo sapiens (human) DGK-epsilon	215	KQWT	PLIILANS	RS	SGTNM	GEGLLGE	FRIL	245	
Homo sapiens (human) DGK-zeta	480	PLMK	PLLVFN	PKSG	GNQGAK	I IQS	FLWY	510	
Homo sapiens (human) DGK-eta	328	FCVS	PLLVFN	SKSG	DNQGVK	FLRR	FKQL	358	
Homo sapiens (human) DGK-theta	584	PDSC	PLLVFN	PKSG	GLKGRD	LLCS	FRKL	614	
Homo sapiens (human) DGK-iota	372	PLMK	PLLVFN	PKSG	GNQGT	KVLQM	FMWY	402	
Homo sapiens (human) DGK-kappa	487	ACSC	PLLI	FINS	SKSG	DHQG	IVFLRK	FKQY	517
Dictyostelium discoideum (social amoeba) DGKA		NFLQ	IIDL	IKCG	GF	DSTL	QMINRYLAKHPE	390	
Homo sapiens (human) DGK-alpha		NFRQ	VFN	LLK	-DGE	EIGL	RRLF	423	
Homo sapiens (human) DGK-beta		NFRQ	VYS	ISG	-NGF	MPLN	NFR	485	
Homo sapiens (human) DGK-gamma		NPKQ	VFN	LDN	-GFF	TPGL	NFR	481	
Homo sapiens (human) DGK-delta		NPAQ	VFD	LMN	-GGF	HLGL	RRLFQ	368	
Homo sapiens (human) DGK-epsilon		NEVQ	VFD	VTK	-TPE	IKAL	QLCTL	268	
Homo sapiens (human) DGK-zeta		NFRQ	VFD	LSQ	-GGF	KEALE	MYR	531	
Homo sapiens (human) DGK-eta		NPAQ	VFD	LMN	-GGF	HLGL	RRLFQ	379	
Homo sapiens (human) DGK-theta		NPHQ	VFD	LTN	-GGF	LPGL	HLFS	635	
Homo sapiens (human) DGK-iota		NFRQ	VFD	LSQ	-EGF	KDALE	LYR	423	
Homo sapiens (human) DGK-kappa		NPSQ	VFD	LLK	-GGF	EAGL	SMPK	538	
Dictyostelium discoideum (social amoeba) DGKA		QTNRF	RI	LV	CGGD	TV	GWLFKQMTKHLV	418	
Homo sapiens (human) DGK-alpha		DVPDS	RI	LV	CGGD	TV	GWILETIDKANL	451	
Homo sapiens (human) DGK-beta		DVPDF	R	VLA	CGGD	TV	GWVLDICIEKANV	513	
Homo sapiens (human) DGK-gamma		DTPDF	R	VLA	CGGD	TV	GWVLDICIDKANF	509	
Homo sapiens (human) DGK-delta		KFDTR	RI	LV	CGGD	SV	GWVLSSEIDSLNL	396	
Homo sapiens (human) DGK-epsilon		PYYSA	R	VLV	CGGD	TV	GWVLDVAVDDMKIKG	298	
Homo sapiens (human) DGK-zeta		KVHNL	R	IL	ACGG	D	TV	GWVLSLTDQLRL	559
Homo sapiens (human) DGK-eta		KFDNF	RI	LV	CGGD	SV	GWVLSSEIDKLN	407	
Homo sapiens (human) DGK-theta		QVPCF	R	VL	CGGD	TV	GWVLGALAEETRYRL	665	
Homo sapiens (human) DGK-iota		KVPNL	R	IL	ACGG	D	TV	GWVLSLDELQL	451
Homo sapiens (human) DGK-kappa		NFARF	RI	LV	CGGD	SV	SWVLSLIDAFGL	566	
Dictyostelium discoideum (social amoeba) DGKA		--PSTI	PIGII	PLGT	GN	DLAR	SLGWGIGYD	446	
Homo sapiens (human) DGK-alpha		--PVL	PPVAV	LPLGT	GN	DLAR	CLRWGGGYE	479	
Homo sapiens (human) DGK-beta		--GKH	PPVAI	LPLGT	GN	DLAR	CLRWGGGYE	541	
Homo sapiens (human) DGK-gamma		--AKH	PPVAV	LPLGT	GN	DLAR	CLRWGGGYE	537	
Homo sapiens (human) DGK-delta		--HKQ	QLGV	LPLGT	GN	DLAR	VLGWGSACD	424	
Homo sapiens (human) DGK-epsilon		QEKY	IPQVAV	LPLGT	GN	DL	SNLWGTGYA	328	
Homo sapiens (human) DGK-zeta		--KPP	PPVAI	LPLGT	GN	DLAR	TNLWGGGYT	587	
Homo sapiens (human) DGK-eta		--NKQ	QLGV	LPLGT	GN	DLAR	VLGWGSYD	435	
Homo sapiens (human) DGK-theta		A-CPE	PSVAI	LPLGT	GN	DL	GRVLRWAGYS	694	
Homo sapiens (human) DGK-iota		--SPQ	PPVGV	LPLGT	GN	DLAR	TNLWGGGYT	479	
Homo sapiens (human) DGK-kappa		--HEK	QLAVI	PLGT	GN	DLAR	VLGWGAFWN	594	
Dictyostelium discoideum (social amoeba) DGKA		GE-KLIE	ILKS	INEAKTIQ	MT	W	SIEMWD	474	
Homo sapiens (human) DGK-alpha		GQ-NLAK	ILK	DLEMSKVVHMD	DRW	SVEVIP	-	507	
Homo sapiens (human) DGK-beta		GE-NLMK	ILK	DIENSTEIML	DRW	KFEVIP	-	569	
Homo sapiens (human) DGK-gamma		GG-SLTK	ILK	DIEQSPLVML	DRW	HLEVIP	-	565	
Homo sapiens (human) DGK-delta		DDTQLP	QILE	EKLERASTKML	DRW	SVMAY	--	452	
Homo sapiens (human) DGK-epsilon		GEIPVA	QVLR	NVMEADGIK	LRW	KVQVTN	-	357	
Homo sapiens (human) DGK-zeta		DE-PVSK	IL	SHVEEGNVVQL	DRW	DLHAE	P-	615	
Homo sapiens (human) DGK-eta		DDTQLP	QILE	EKLERASTKML	DRW	SIMTYE	-	464	
Homo sapiens (human) DGK-theta		GE-DPFS	VLLS	VDEADVLM	DRW	TILLDA	-	722	
Homo sapiens (human) DGK-iota		DE-PVSK	IL	CQVEDGTVVQL	DRW	NLHVERN	-	508	
Homo sapiens (human) DGK-kappa		KSKSP	PLDIL	NRVEQASVRI	LRW	SVMIRE	-	623	

Fig. S2. Conservation of the DGK catalytic region between *D. discoideum* and all *H. sapiens*

isoforms. Sequence alignment of the catalytic site of *D. discoideum* DGKA and the 10 *H. sapiens* DGK isoforms. The names of the species and DGK isoforms used for comparison in the alignment are shown to the left with the amino acid start and end position in the protein shown at the start and end of the sequence respectively. Identical amino acids are highlighted in blue.

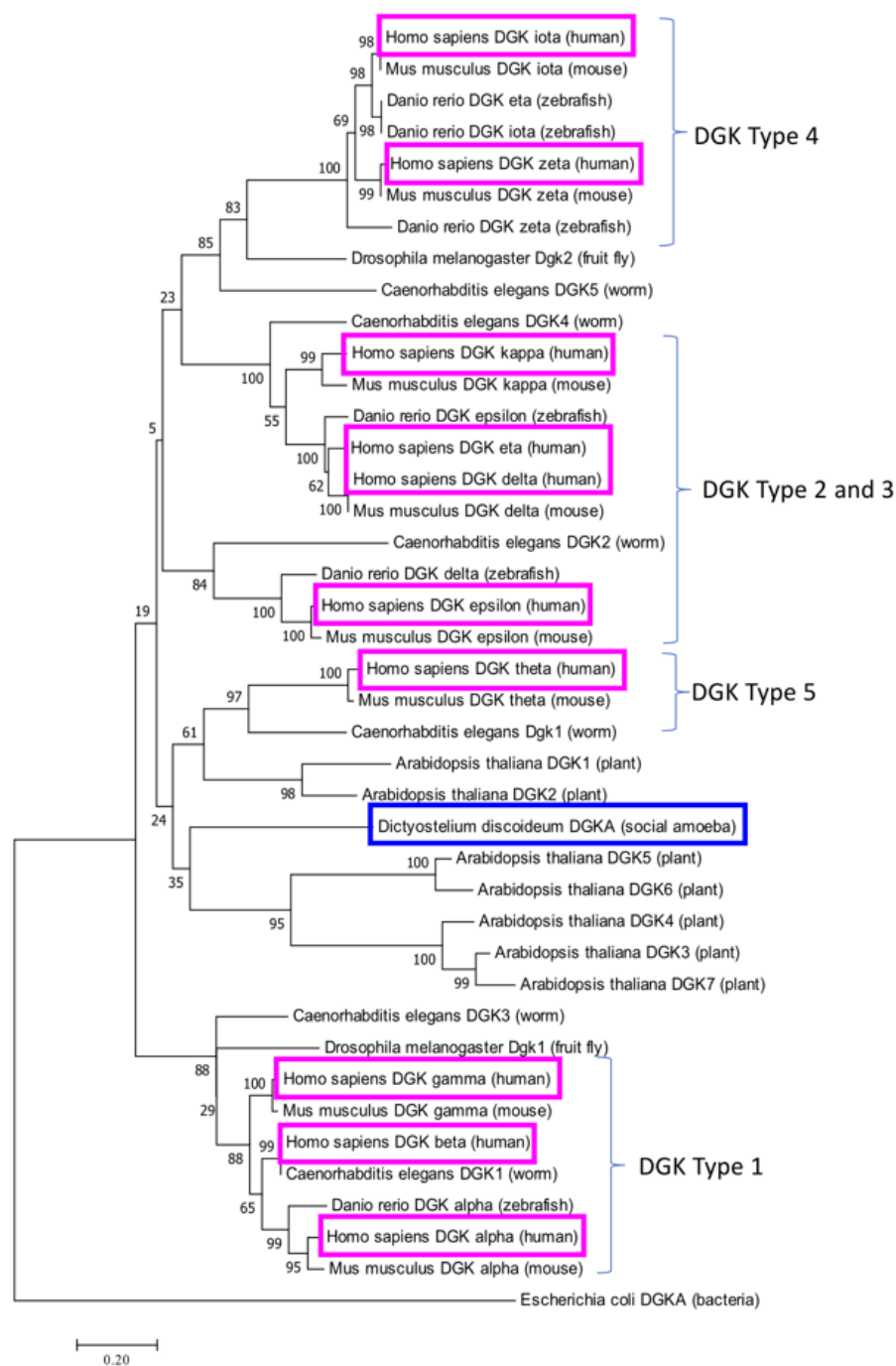


Fig. S3. Phylogenetic analysis of DGK proteins within a range of kingdoms. A Bootstrap consensus tree showing the evolutionary conservation of DGK generated using the Molecular Evolutionary Genetic Analysis (MEGA) 7 software neighbour-joining method with Bootstrap test (500 replicates) and the Poisson correction method to compute the evolutionary distances. Numbers on the tree represent the percentage of replicate trees in which the associated taxa are clustered together. *E. coli* DGKA represents the root of the tree. Human isoforms are highlighted in pink, with the *Dictyostelium* protein highlighted in blue.

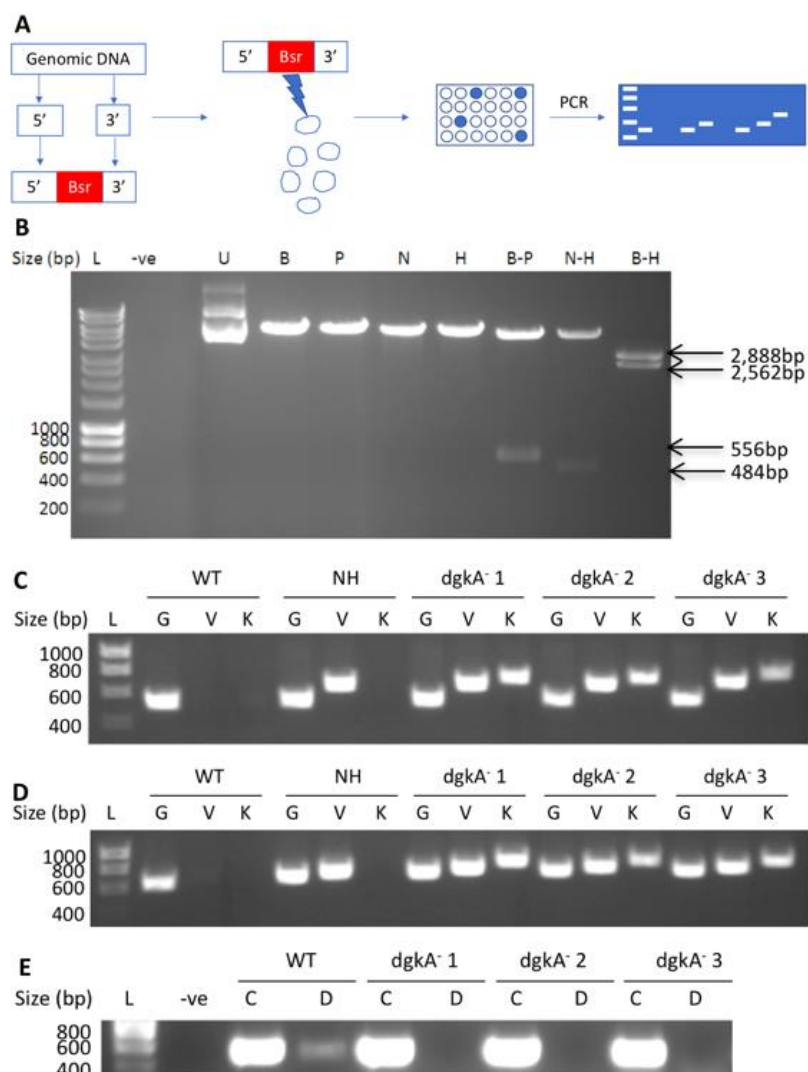


Fig. S4. Creation of *dgkA* knockout cassette and *dgkA*⁻ *Dictyostelium* cell lines. (A) Schematic of creating *dgkA* knockout cell lines where two fragments of genomic DNA sequence were PCR amplified and inserted either side of a blasticidin resistance gene, creating a knockout cassette which was electroporated into WT Ax2 *Dictyostelium* cells where transformant cell lines were selected by blasticidin and surviving knockout cell lines were confirmed by PCR. (B) Confirmation of the two *dgkA* genomic DNA inserts in the pLPBLP vector by a series of restriction digests run on a 1% agarose gel by electrophoresis using a 1kb DNA hyperladder (L), uncut knockout vector (U), single digests to confirm individual enzyme activity of BamHI (B), PstI (P), NcoI (N) and HindIII (H) and double digests of BamHI-PstI (B-P) and NcoI-HindIII (N-H) to confirm the presence of the 5' and 3' fragments and BamHI-HindIII (B-H) which excise the linearised knockout fragment used for electroporation. Homologous intergration screening PCR gel electrophoresis of the genomic control (G), vector control (V) and knockout diagnostic (KO) PCR products where WT would only have the genomic control, non-homologous intergrants (NH) the genomic and vector control bands and homologous intergrants

(*dgkA*⁻) would have all three bands at the N (**C**) and C (**D**) terminal regions. (**E**) RT-PCR gel electrophoresis confirming the presence of the housekeeping gene Ig7 (C) in both WT and *dgkA*⁻ cell lines and the absence of deleted region (D) only in the *dgkA*⁻ cell lines.

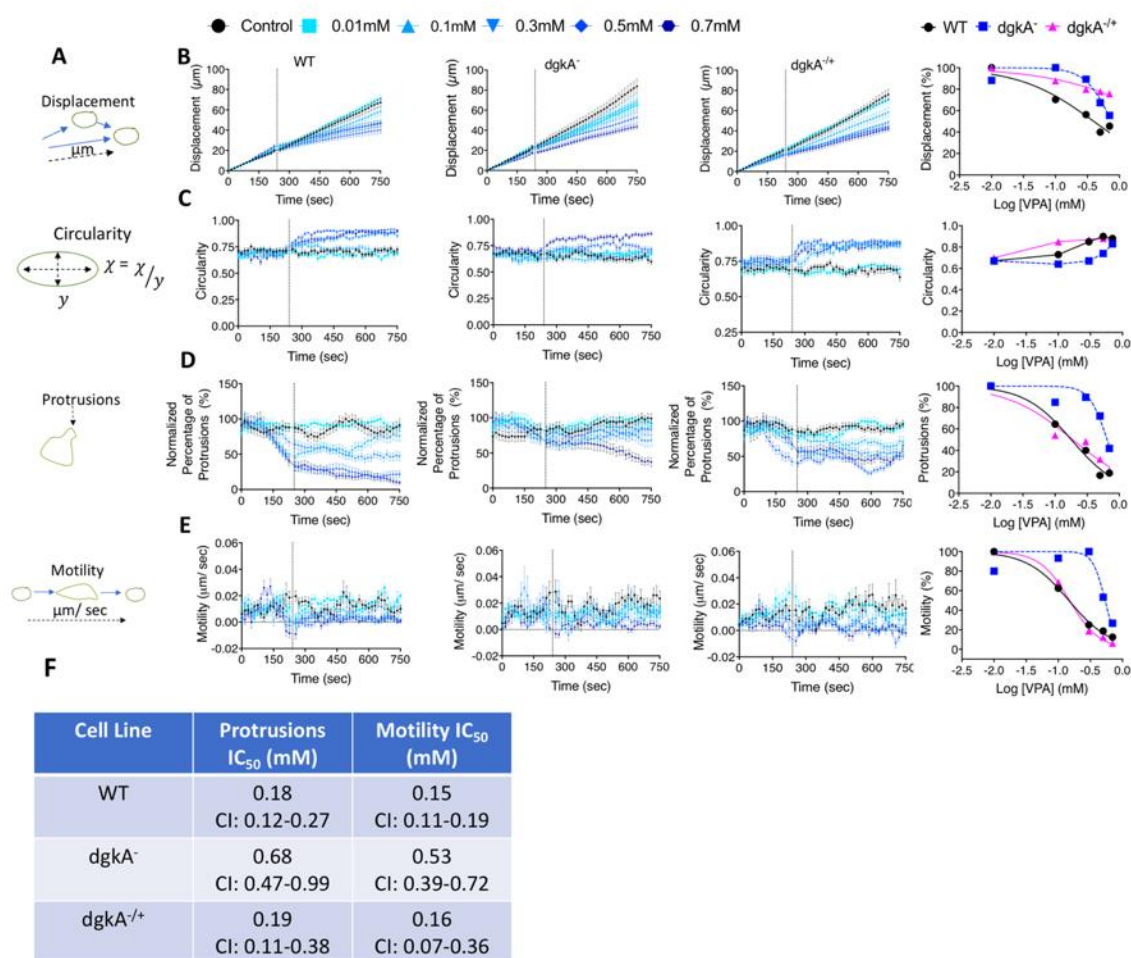


Fig. S5. *dgkA*^{+/-} has restored acute cell response phenotype when exposed to VPA. (A) Quantification of cell displacement, circularity, percentage of protrusions and motility in the absence and presence of a range of VPA concentrations (0.01mM to 0.7mM) in WT Ax2, *dgkA*⁻ and *dgkA*^{+/-} cells. (B) Calculated IC₅₀ values for WT, *dgkA*⁻ and *dgkA*^{+/-} cell lines for protrusions and motility. Data presented as mean (+/- SEM), *n* = 30 cells. A Kruskal- Wallis with Dunns post hoc test was used to compare WT, *dgkA*⁻ and *dgkA*^{+/-} cell lines where there was significant differences in WT cell and *dgkA*⁻ cell (black stars) displacement (0.1mM, 0.3mM and 0.5mM VPA), circularity (0.3mM VPA), protrusions (0.3mM and 0.5mM VPA) and motility (0.3mM VPA); WT cell and *dgkA*^{+/-} (pink stars) displacement (0.5mM); and between *dgkA*⁻ and *dgkA*^{+/-} (blue stars) displacement (0.1mM), circularity (0.1mM, 0.3mM and 0.5mM), protrusions (0.3mM) and motility (0.3mM). *P* value: * *P* value = <0.05, ** *P* value = <0.01, *** *P* value = 0.01 and **** *P* value = < 0.001.